# Si/SiGe Quantum Devices and Quantum Wells: Electron Spin Coherence

J. L. Truitt[1], K. A. Slinker[1], K. L. M. Lewis[1], D. E. Savage[1], Charles Tahan[2], L. J. Klein[1], J. O. Chu[3], P. M. Mooney[4], A. M. Tyryshkin[5], D. W. van der Weide[6], M. G. Lagally[7], Robert Joynt[1], S. N. Coppersmith[1], Mark Friesen[1], and M. A. Eriksson[1]

[1] Department of Physics, University of Wisconsin, Madison, Wisconsin 53706, USA
[2] Cavendish Laboratory, Madingly Road, Cambridge CB3 OHE, UK
[3] IBM Research Division, T. J. Watson Research Center, New York 10598, USA
[4] Department of Physics, Simon Fraser University, Burnaby, BC V5A 1S6, Canada
[5] Department of Electrical Engineering, Princeton University, Princeton, New Jersey 08544, USA
[6] Department of Electrical and Computer Engineering, University of Wisconsin, Madison, Wisconsin 53706, USA
[7] Department of Materials Science and Engineering, University of Wisconsin, Madison, Wisconsin 53706, USA

## 1 Introduction

Quantum devices are presently an area of intense activity. This is due in part to novel computing opportunities offered by quantum computing and quantum information more generally, and in part by the need to control quantum effects in classical devices. It also underscores a new era of technology, in which it has become possible to control the fundamental quantum degrees of freedom of microscopic objects, even within the confines of a solid-state matrix. Electron spins form an excellent basis for quantum devices, since they may be isolated in quantum dots, artificial or natural, and in principle they can transported to distant locations through quantum channels. The spin variable can be controlled through either electric or magnetic fields [1].

The main challenge for spintronics applications is to manipulate and measure the spins, while simultaneously isolating them from their environment. The degradation of spin information is known as decoherence. In the semiclassical spin field effect transistor (SFET) [2], decoherence leads to diminished functionality of the device, while for spin qubits, decoherence leads to computing errors [3]. Decoherence properties may depend on fundamental materials properties, growth conditions, temperature, or any number of environmental variables. The study of decoherence properties of spins has a long and venera-

ble history in solid-state physics, and a number of powerful probe techniques have been established. Preeminent among these is spin resonance, for example electron spin resonance (ESR) [4] or nuclear magnetic resonance (NMR) [5]. Many variations on these techniques have been developed. Quantum devices provide a challenge for such bulk techniques, since the number of active electrons may be very few. In this case, electrically detected ESR techniques (ED-ESR) play an important role [6]. In the limit of single-electron devices, completely new methods are required, based on single-spin manipulation and readout [7–14].

While many recent advances in quantum devices have occurred in the GaAs materials system, silicon occupies a unique position. On the one hand, the materials environment of silicon has the distinction of having the smallest spin-orbit coupling of any currently practical semiconducting material, due to its high position in the periodic table. Additionally, the predominant isotope of silicon is $^{28}$Si, with nuclear spin zero. Modulation-doping, isotopic purification, and clean heterostructures therefore hold the prospect of an environment with very low decoherence. On the other hand, Si quantum wells are clad by SiGe barriers, and therefore intrinsically strained, leading to growth and fabrication challenges. Moreover, as an indirect bandgap material, the conduction band structure of silicon is fundamentally more complicated than that of direct gap materials, leading to decoherence and spin manipulation challenges associated with multiple conduction valleys.

In this paper, we review the decoherence properties of electron spins in silicon structures, with a focus on materials appropriate for few-electron quantum devices. While it is likely that single electron measurements similar to those in GaAs will be available in the near future, it is also urgent to understand the dominant decoherence sources in transport experiments involving many electrons. Below, we review the current status of silicon quantum devices, particularly those of importance for spin electronics (spintronics) and quantum computing. In addition to spin physics, we consider the special behavior of silicon devices related to valley physics. We also review the current status of ESR experiments in Si/SiGe quantum wells.

Many factors can effect transport in silicon devices, including variable germanium content in the quantum well and the barriers, use of oxide materials as barriers, proximity of modulation doping layers and their impurity ions, presence of dopants in the quantum well, width of the quantum well, and roughness of the interfaces. It is therefore important to test current theories of scattering in a variety of devices and samples. In the second half of our paper, we present preliminary data obtained from several different samples which have been recently used in the fabrication of quantum devices, including quantum point contacts and few-electron quantum dots. Based on transport data through these devices, we deduce that they are of very high quality. However, the samples are not of the same origin as those used in many recent ESR experiments. We find that while some of the samples show similar ESR behavior as previous experiments, others show differences that

cannot be fully explained by existing theories. We conclude that the current understanding of Si structures, especially those of importance for quantum devices, is not yet complete.


## 2 Silicon Quantum Devices

Many high performance devices in silicon, from microchips to qubits, are fabricated in two-dimensional structures, including inversion layers and quantum wells. Inversion layers have traditionally been of the greatest importance for commercial electronics, taking the form of metal oxide semiconductor field effect transistors (MOSFETs), with the active region an inversion layer at the silicon/silicon-dioxide interface. Because of their industrial importance, inversion layers have been extensively studied. A great wealth of knowledge about such structures and the devices formed on them can be found in the review paper of Ando, Fowler and Stern [15], and other texts [16].

Silicon quantum devices can be made using oxidation fabrication techniques, frequently in combination with silicon-on-insulator (SOI) structures. Much research in silicon single electron transistors (SETs) has focused on high temperature quantum dots [17–19]. However, a burst of activity on low-temperature quantum devices, with an emphasis on qubit development, has broadened the direction of recent fundamental research. This work covers a range of topics, including coulomb blockade effects [20], single electron memories [21], control of electron density by top-gates [22], and fine tuning of tunnel barrier resistances [23]. The resulting devices have attained a high degree of sophistication, leading to quantum dots strongly coupled to charge sensors [24], triple dots [25], spin effects in coupled dots [26], and single hole transfer devices [27].

Several variations on the MOSFET design have arisen, in some cases yielding better performance for quantum devices. Of particular interest is the doped $SiO_2/Si/SiO_2$ quantum well. Devices fabricated in such structures include double dot charge qubits with strongly coupled charge sensors [28]. The quality of the quantum wells may be very high, enabling electrically detected electron spin resonance with enough resolution to detect valley splitting [29]. (Further discussion is given below.) However, low temperature mobilities in these structures are typically on the order of $10^4 \, cm^2/Vs$ or lower [29]. Moreover, rough interfaces associated with oxide barriers may have a detrimental effect on electronic properties, especially in ultrathin quantum wells [30], and the electrostatic potentials from ionized dopants in the quantum well may interfere with device operation [31].

There are pros and cons in utilizing $Si/SiO_2$ interfaces for quantum devices. Silicon quantum dots created by oxidation may be extremely stable [32]. There has nonetheless been concern about ubiquitous defects at the interface between crystalline and non-crystalline materials [33–37]. In the very

best oxide-silicon interfaces, defect densities can be very low indeed, suggesting that the challenges are not insurmountable. The preceding summary of Si/SiO$_2$ materials and devices is not meant to be exhaustive, since these structures are not the focus of the present work. For a more thorough treatment, we direct the reader elsewhere [15, 16, 38].

The Si/SiGe heterostructure is the main focus of this paper. To form a two-dimensional electron gas (2DEG), a narrow silicon layer is clad within strain-relaxed SiGe barriers, causing tensile strain in the silicon [39]. Similarly, a hole gas is formed in a SiGe quantum well clad within silicon barriers. A review of growth issues in silicon/germanium materials is given in [40].

Highly doped Si/SiGe quantum wells have been successfully used to create quantum dots and double dots, both in $p$-type [41–43] and $n$-type [44,45] materials. However, modulation doping can also be achieved in Si/SiGe heterostructures. The resulting structures are analogous to the epitaxial GaAs/AlGaAs structures, which have been utilized in a range of quantum devices of sufficient quality to form spin qubits [7–14]. One main difference between Si- and GaAs-based devices is strain, which occurs in the Si structures. Modulation doped field effect transistors (MODFETs) or high electron mobility transistors (HEMTs) are expected to provide a factor of three improvement in mobilities over MOSFETs at room temperature [39], and even more improvement at low temperatures. Since the mid-1990's, silicon MODFETs have been optimized to provide mobilities in excess of 600,000 cm$^2$/Vs. [39, 46–50]. For qubit devices, which do not utilize transport, there is no conclusive data that high mobilities correlate with desirable properties for quantum computing. However, existing qubits in GaAs utilize ulta-high mobility materials [7–9, 11], and it is anticipated that the same materials issues that reduce the mobility, such as remote impurities, or scattering centers in the quantum well or oxide interface, could also adversely affect qubit performance. In SiGe MODFETs, the primary scattering centers in ultra-high mobility materials are remote ionized impurities in the doping layer [39, 51, 52]. However, other scattering centers include rough interfaces in the quantum well, which arise from misfit dislocation formed during strained growth, even when no threading dislocations are present in the quantum well [40].

Quantum devices in silicon/silicon-germanium quantum wells have been reviewed in Ref. [53]. To form quantum dots in Si/SiGe quantum wells, lateral confinement can be produced by physical means, using lithographic and etching techniques to carve up the 2DEG [54, 55]. A more versatile technique uses nanoscale metallic gates to electrostatically deplete the 2DEG, analogous to techniques used in GaAs devices [56]. Optimally, these finger gates are fabricated on the surface of the heterostructure directly above the 2DEG, at a separation of about 50 nm. A primary challenge for creating top-gates in silicon arises from the presence of leakage paths [57], which may result from threading dislocations, deep pits, or other morphological features associated with strained growth [58]. The leakage mechanisms may also vary for different growth methods [59]. Dislocations are generally harmful for electrical prop-

erties in the 2DEG. Fortunately, optimization of growth methods has shown that the number of defects can be minimized in the active layer. Since the absence of leakage is prerequisite for good quantum devices, this area of research progressed rather slowly for several years, until the aforementioned difficulties were resolved.

One possibility for eliminating leakage is to avoid top-gates altogether, by replacing them with side-gates. The side gates are formed within the same 2DEG as the active device, but they are electrically isolated by means of reactive ion etching [60–62], in analogy with SOI-based devices. The etching provides confinement in one direction, allowing the formation of quantum wires [58, 63–65]. In combination with electrostatic gates, this technique enables electrical control of the tunnel barriers, which may be used to form quantum point contacts [66] and quantum dots [57, 62, 67, 68]. However, some drawbacks of side-gating are large gate widths (compared with top-gates), resulting in reduced gate density, and increased gate distance, which limits the fine-tuning of gate-defined device features. A possible solution to this problem is to utilize metal gates fabricated within the etch trench [69]. This avoids the problem of leakage, while aligning the gates more closely with the quantum dot.

Difficulties in forming Schottky top-gates have recently been overcome. Starting in the 1990's, it was shown that Schottky gates could modulate electron densities in 2DEGs [70, 71]. It is now possible to fabricate top-gated quantum dots be a number of different methods, including heterostructure optimization [72, 73], etching the surface to remove near-surface highly doped regions [74].

Top-gated Si/SiGe quantum dots formed in 2DEGs have now been developed to the point that quantum effects such as Fano and Kondo resonances are now observed [73]. Top-gates can also be used to create quantum point contacts [59, 66, 75–78]. Such point contacts have recently been used to enable spectroscopy of valley states in Si/SiGe 2DEGs [79].

An interesting recent approach to Si/SiGe heterostructure growth may provide an alternative route to forming robust Schottky gates. In [80] and [81], quantum wells were formed by strain-sharing growth methods, on top of an SOI substrate. In such structures, dislocations are entirely absent, since the structure is thinner than the critical thickness for dislocation formation. Strain sharing is accomplished by under-etching the membrane, floating it off the substrate, and redepositing it on a new substrate. Transport measurements demonstrate the presence of a 2DEG. Such alternative growth methods may result in structures that are free of the types of roughness and defects that accompany conventional strained growths.

## 3 Spins and Valleys

Much of the recent interest in silicon quantum devices was initiated by the quantum dot spin qubit proposal by Loss and Di Vincenzo [82]. (Recent progress is reviewed in [83].) Kane [84] has discussed the advantages of working in silicon, and further innovations of using donor nuclear spin qubits have been presented [85–89]. A similar donor-bound approach can be extended to electron spin qubits [90–93]. Vrijen et al. [94] have made a further extension to silicon-germanium heterostructures. Schemes have also been proposed for electron spin-based quantum computation in silicon-germanium quantum dots [95, 96].

Spin decoherence mechanisms are of fundamental importance for spin-based quantum devices, and more generally for spintronics [1]. Silicon is an excellent model system for studies of decoherence, and electron spins in silicon have long coherence times [97], making them particularly attractive for applications. When nuclear spins are present, the electron phase relaxation time $T_M$ for phosphorus-bound donor electrons is dominated by spectral diffusion due to flip-flops of the host nuclear spins [98]. However, the isotopic purification of silicon's naturally abundant, spin-zero nuclear isotope $^{28}$Si leads to orders of magnitude improvement. In the latter case, the electron spin decoherence time $T_2$ has been measured to be as long as 14 ms at 7 K, and extrapolates to on the order of 60 ms for an isolated spin [99]. While it has so far been possible to detect spin resonance in specialized silicon structures [100], and while spin coherence has been observed in quantum dots [73], there have not yet been reports of spin qubits in silicon quantum devices. Following recent progress in GaAs [7, 13, 14], including few-electron decoherence measurements [8–12].

An important distinction between silicon and GaAs quantum devices is in the low-lying valley structure of their conduction bands. As an indirect gap semiconductor, bulk silicon exhibits six degenerate valleys, which may compete with spin as a quantum variable for quantum computing applications [53, 101]. The valley degree of freedom is very important in low-temperature, quantum devices, leading to a recent resurgence of interest in the subject of valley splitting, as we now explain.

In a silicon inversion layer or quantum well, only two valleys will be populated [the $\pm z$ valleys, for silicon (001)]. The degeneracy of these valleys is broken in the presence of a sharp quantum well interface. The value of this valley splitting, and its importance for experiments has been a subject of interest for many years, beginning with the surface scattering theory of Sham and Nakayama [102], the "electric breakthrough" theory of Ohkawa and Uemura [103–105], and other formulations [106–109]. More recently, powerful tight-binding methods [110–113] and effective mass theories [101, 113, 114] have provided new insights.

A crucial question is whether valley splitting is large enough to allow a workable spin qubit Hilbert space. A number of experimental papers have measured valley splitting as a function of magnetic field [29, 115–122], finding

surprisingly small values of the splitting, which would not enable spin qubits. However, the significance of atomic steps due to quantum wells grown on miscut substrates, or, more generally, in the presence of interfacial roughness has recently been shown to cause a large reduction of the valley splitting [79, 114, 123–125]. Lateral confinement lifts this suppression, allowing valley splitting to approach its theoretical upper bound [79]. Valley splitting is also found to approach the theoretical upper bound in $SiO_2/Si/SiO_2$ quantum wells [29, 30, 126]. In this case, because of the narrow quantum wells and the sharp potential barriers, the valley splitting reaches large values, on the order of 20 meV. Because of the dependence of valley splitting on lateral confinement, quantum devices like quantum point contacts have become an important new tool in the study of valley splitting [75, 76, 79].

## 4 ESR in Silicon Quantum Wells

While for qubit applications one must be concerned with spin relaxation of localized spins, the transport of spin information over long distances is important for many spintronics applications. Interestingly, the mechanisms for spin relaxation of electrons with extended wavefunctions are quite different than those of localized electrons. Delocalized electrons undergo momentum scattering. D'yakonov and Perel' (DP) pointed out in the early 1970's that such scattering of electrons gives rise to spin relaxation in the presence of spin-orbit coupling [127]. This DP mechanism dominates spin relaxation at low temperatures in two-dimensional electron gases in GaAs heterostructures [128]. It also dominates the field-independent part of the relaxation at intermediate temperatures in bulk GaAs [129, 130]. In addition to the advantage of naturally abundant nuclear spin-zero isotopes, noted above, silicon also has much weaker spin-orbit coupling than GaAs, and the DP mechanism is therefore not as significant. Nevertheless, it is expected to dominate the relaxation in two-dimensional electron gases in Si 2DEGs.

There have been a number of studies of electron spin coherence in Si/SiGe 2DEGs over the last decade, as well as measurements on related $X$-valley systems [131, 132]. A principle measurement technique is ED-ESR [133], which is of importance because of the reduced number of spins in the 2DEG compared with bulk. The signal in this case is obtained from conductivity measurements, and arises mainly from the reduction of spin polarization, rather than electron heating [134]. ED-ESR can be extended to provide information on valley splitting as well, in which case it is known as EVR [79]. Sharp ESR resonances in Si/SiGe 2DEGs also allow for standard microwave absorption measurements of as few as $10^9$ spins [135–137].

Early ESR measurements demonstrated the importance of potential fluctuations caused by ionized donors in the doping layer [135–137], which are also thought to play a leading role in limiting the mobility in these devices [39, 51, 52]. Indeed, mobility calculations, based on an ESR density of

states analysis of the potential fluctuations, provide good agreement with experimental values [138].

The ESR data exhibit anisotropy with respect to the magnetic field direction in both the linewidth (dephasing time) and the electron $g$-factor [133, 139, 140]. This behavior suggests Bychkov-Rashba spin-orbit coupling as an origin for DP-mediated spin relaxation. Wilamowski and coworkers have proposed an additional modulation of the spin-orbit coupling and the ESR signal, originating from the motional narrowing due to cyclotron motion [141, 142]. The anisotropy is also affected by the germanium content in the quantum well [143, 144] and the electric current [145], providing mechanism for $g$-factor tuning in these systems.

ESR measurements provide several crucial estimates of device parameters in the Si/SiGe quantum well. Wilamowski *et al.* obtain the Bychkov-Rashba spin-orbit coupling parameter $\alpha = 0.55 \times 10^{-12}$ eV cm [139, 140]. Graeff et al. obtain the anisotropic $g$-factors $g_{\parallel} = 2.0007$ and $g_{\perp} = 1.9999$ for the 2DEG charge density of $n = 4 \times 10^{11}\,\text{cm}^{-2}$. Pulsed measurements suggest spin coherence ($T_2$) times up to $3\,\mu\text{sec}$ [146]. The latter may be enhanced by confinement effects [144]. The longitudinal spin relaxation time is strongly enhanced by in-plane magnetic fields, giving $T_1$ on the order of 1 ms in a 3.55 T field [134].

In the remainder of this paper we revisit the issue of linewidth anisotropy. We specifically consider several of the same heterostructures that were used to fabricate quantum devices [57, 62, 72, 73, 79]. We provide a comprehensive treatment of six different samples, using transport measurements to extract the electron density and scattering time. We use ESR to measure $T_2^*$ and to provide an indication of the spin decoherence mechanism. A detailed study indicates that the dominant decoherence mechanism is strongly dependent on the orientation of the magnetic field — so much so that it is inconsistent with mechanisms described in the papers described above. Our main conclusions are presented in Table 1.

## 5 Samples

The Si/SiGe heterostructures are grown by ultrahigh vacuum chemical vapor deposition at the University of Wisconsin - Madison and at IBM-Watson [48]. The 2DEG sits near the top of a strained Si layer grown on a strain-relaxed $Si_{1-x}Ge_x$ buffer layer, as shown in Fig. 1(a) of [57]. Above the 2DEG is a $Si_{1-x}Ge_x$ offset layer, followed by a phosphorus-doped dopant layer, and then a $Si_{1-x}Ge_x$ spacer layer capped with Si at the surface. Table 1 contains the heterostructure details for each sample.

Hall measurements are performed on each sample. The Hall bars are fabricated by etching and Ohmic contacts are made to the 2DEG by Au/Sb metal evaporation and annealing at 400°C for 10 minutes. The Hall data are used to extract the electron density and mobility. From the mobility we derive the

**Table 1.** Sample parameters and measurements of six $Si_{1-x}Ge_x/Si/Si_{1-x}Ge_x$ quantum wells. The first section of the table contains growth parameters: quantum well width, germanium composition of the barriers $(x)$, dopant offset distance, doping layer thickness, spacer layer thickness, and capping layer thickness. The next section contains results from Hall transport measurements: 2DEG charge density $(n_e)$, mobility $(\mu)$ and momentum relaxation time $(\tau_p)$. The last three columns contain ESR results: $T_2^*$ is derived from (1), using $g = 2.00$ for all samples, $A(15°)$ is the anisotropy parameter corresponding to the magnetic field orientation $\theta = 15°$, as described in (3), and $b$ is the fitted quadratic coefficient of the anisotropy, from (4)

| Sample | well width (nm) | $x$ | offset (nm) | dopants (nm) | spacer (nm) | cap (nm) | $n_e$ ($10^{11}$ cm$^{-2}$) | $\mu$ (cm$^2$/Vs) | $\tau_p$ (ps) | $T_2^*$ ($\mu$s) | $A(15°)$ | $b$ (rad$^{-2}$) |
|---|---|---|---|---|---|---|---|---|---|---|---|---|
| ibm-01 | 8.0 | 0.30 | 14 | 1 | 14 | 3.5 | 4.0 | 37,300 | 4.3 | 0.6 | 1.0 | 1.6 |
| uw-030827 | 10 | 0.35 | 15 | 22 | 35 | 10 | 4.8 | 90,000 | 9.7 | 0.1 | 4.7 | 38 |
| uw-030903 | 10 | 0.25 | 13 | 17 | 35 | 10 | 4.3 | 86,700 | 9.4 | 0.2 | 2.1 | 13 |
| uw-031121 | 10 | 0.30 | 20 | 6 | 60 | 20 | 5.4 | 38,000 | 5.0 | 0.1 | 2.0 | 25 |
| uw-031124 | 10 | 0.30 | 20 | 26 | 40 | 20 | 4.7 | 63,200 | 6.9 | 0.1 | 2.0 | 18 |
| uw-031203 | 10 | 0.30 | 60 | 6 | 60 | 20 | 2.6 | 17,100 | 1.8 | 0.5 | 2.3 | 10 |

momentum relaxation time $\tau_p = m_e^*\mu/e$, an important parameter in spin relaxation via spin-orbit and related interactions. The parameters reported in Table 1 have been corrected for a small parallel conduction path using the method of Kane et al.,[1] and in each case this correction was smaller than 1% [147].

## 6 ESR Measurements

Electron spin resonance data were acquired with a Bruker ESP300E X-band spectrometer, using an Oxford Instruments ESR900 continuous flow cryostat to maintain a sample temperature of 4.2 K. Magnetic field calibration and tracking was done with an ER035M NMR Gaussmeter. The power dependence was checked to ensure the experiments were performed at low enough power that the peak width did not depend on the power level.

---

[1] The unchanging slope of the transverse resistance shows that the conductivity of the parallel conduction path is much less than the conductivity of the 2DEG. This limit is consistent with Kane's analysis, allowing us to extract the 2DEG mobility and electron density as well as the conductivity of the parallel conduction path.
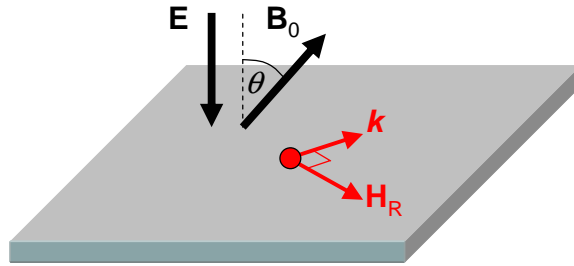
**Fig. 1.** Electrons in the quantum well move in the presence of a modulation doping field. As a consequence of relativity, they then experience an effective in-plane magnetic field $H_R$, known as the Rashba field, in addition to an external magnetic field $\mathbf{B}_0$, which is oriented at angle $\theta$ from the normal direction

The ESR spectra for all samples were measured as a function of the orientation of the applied magnetic field, given by the angle $\theta$ between the magnetic field and the growth direction of the sample, as shown in Fig. 1. Figures 2(a) and (c) describe two-dimensional maps of the ESR intensity as a function of magnetic field and orientation angle for two selected samples. The peak-to-peak ESR linewidths $\Delta H_{\mathrm{pp}}$ were extracted by fitting the lineshapes to the derivative of a Lorentzian, as shown in the insets of Figs. 2(b) and (d). The linewidths exhibit a pronounced dependence on the orientation angle $\theta$ as shown in Figs. 2(b) and (d). The minimal ESR linewidths (at $\theta = 0$) and the observed linewidth anisotropies are summarized in Table 1, based on the analysis described below.[2]

## 7 Decoherence Analysis

The ESR linewidth $\Delta H_{\mathrm{pp}}$ is directly related to the coherence time $T_2^*$ through the expression [4]

$$\Delta H_{\mathrm{pp}} = \frac{2}{\sqrt{3}} \frac{\hbar}{g\mu_B} \left( \frac{1}{T_2^*} \right), \tag{1}$$

where $g$ is the Landé $g$-factor and $\mu_B$ is the Bohr magneton. It has been proposed [141] that the orientational dependence of $T_2^*$ (and thus of $\Delta H_{\mathrm{pp}}$)

---

[2]In many ESR data sets, including the inset of Fig. 2(b), there is a small peak near 3341 G, in the region of Landé $g$-factor, $g \approx 2.0$. The peak shows no orientational dependence, and it is wider than the 2DEG peak. Because the peak is almost perfectly equidistant between two 42 G split phosphorous peaks (not shown in the figure), we deduce that it arises from electrons in the dopant layer, which are shared among clusters of phosphorous nuclei. For example, see [148], especially Figs. 15 and 16.
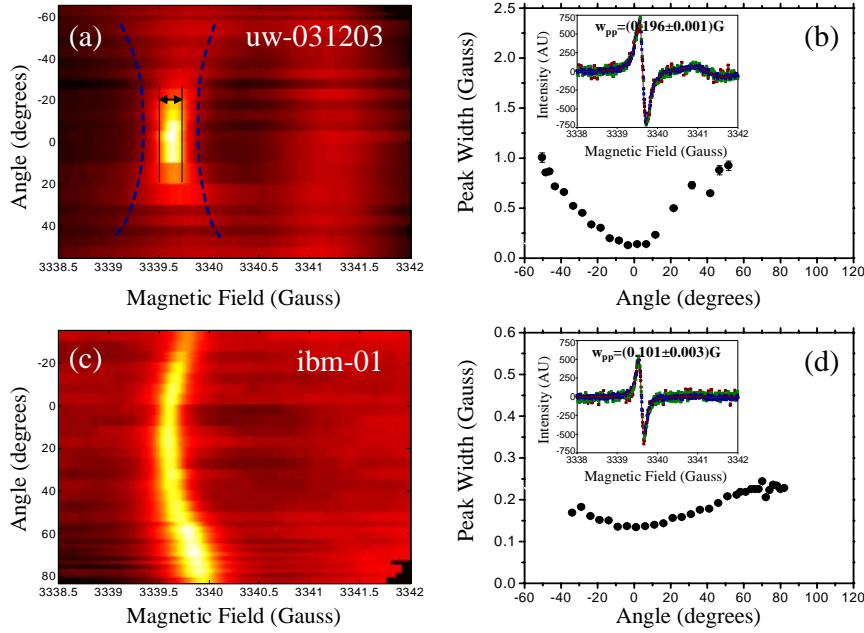
**Fig. 2.** Orientation map of the ESR signal from (**a**) sample uw-031203 and (**c**) sample ibm-01. The color scale describes the peak intensity. The angle on the vertical axis is explained in Fig. 1. Lorentzian fits to the peak width are shown in (**b**) and (**d**) for the same two samples (see inset), as a function of the field angle

in similar 2DEG structures results from a D'yakonov-Perel' spin relaxation mechanism due to fluctuating Rashba fields [127]. There is an electric field perpendicular to the plane of the 2DEG, due to ionized donors in the doping layer, or other interface effects. As a consequence of relativity, mobile electrons in the quantum well then experience an effective magnetic field in the plane of the 2DEG called the Rashba field $H_{\mathrm{R}}$. (See Fig. 1.) Two-dimensional scattering processes therefore induce a fluctuating field $\Delta H_{\mathrm{R}}$ in the 2DEG plane. When the external magnetic field $\mathbf{B}_0$ is perpendicular to the 2DEG ($\theta = 0$), the fluctuating $\Delta H_{\mathrm{R}}$ is perpendicular to $\mathbf{B}_0$. However, when $\mathbf{B}_0$ is tilted with respect to the 2DEG ($\theta \neq 0$), a component of the fluctuating field appears along $\mathbf{B}_0$, resulting in an orientational dependence of $T_2^*$. In general, there may be other contributions to the linewidth, due to inhomogeneous broadening or other decoherence mechanisms, so that the spin coherence time $T_2^*$ may be written as

$$\frac{1}{T_2^*} = \frac{1}{T_{2\mathrm{R}}} + \frac{1}{T_2'},$$
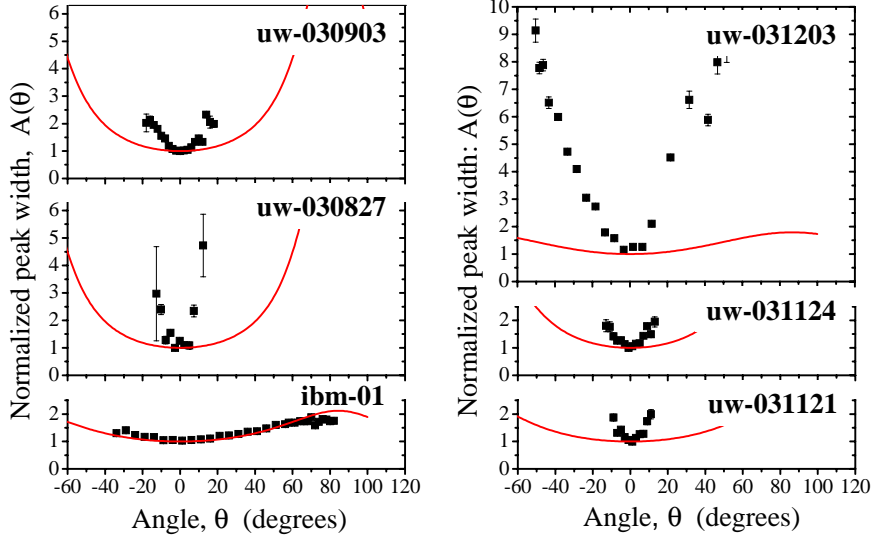
**Fig. 3.** Normalized experimental peak widths are presented as a function of the magnetic field orientation $\theta$, for all six samples. The corresponding theoretical predictions for the anisotropy parameter $A(\theta)$ in (3) are shown as lines, using $\eta = 1/2$

where $1/T_{2R}$ is the Rashba contribution, and $1/T_2'$ includes all other contributions.

Two groups have derived expressions for $T_{2R}$ in the limit $\omega_c \tau_p \cos\theta \gg 1$. Both results can be written in similar fashion as

$$\frac{1}{T_{2R}} = \alpha^2 k_F^2 \tau_p \left[ \frac{\eta}{1 + (\omega_c \cos\theta)^2 \tau_p^2} \sin^2\theta \right.$$
$$\left. + \frac{1/2}{1 + (\omega_L - \omega_c \cos\theta)^2 \tau_p^2} \left( \cos^2\theta + 1 \right) \right]. \qquad (2)$$

The coefficient $\eta = 1/2$ was obtained in [141], while $\eta = 2$ was obtained in [149]. The Rashba coefficient $\alpha$ is defined in the Rashba Hamiltonian $\mathcal{H} = \alpha(\boldsymbol{\sigma} \times \boldsymbol{k}_F) \cdot \hat{\boldsymbol{n}}$, where $\boldsymbol{\sigma}$ are the Pauli spin matrices, $\boldsymbol{k}_F$ is the Fermi wavevector of the electron, $\omega_c = eB/m_e^*$ is the cyclotron frequency, and $\omega_L = g\mu_B H/\hbar$ is the Larmor spin precession frequency [141]. The limit $\omega_c \tau_p \cos\theta \gg 1$ implies that (2) is valid only for small angles $\theta$.

If $1/T_{2R}$ is the dominant term in $1/T_2^*$, then (2) can be normalized to give the anisotropy parameter $A(\theta)$, which depends on the momentum scattering time $\tau_p$, but not the Rashba parameter $\alpha$:[3]

---

[3]The presumed origin of the Rashba field in these samples is from asymmetries occurring in the heterostructure, which lead to internal electric fields. There are four
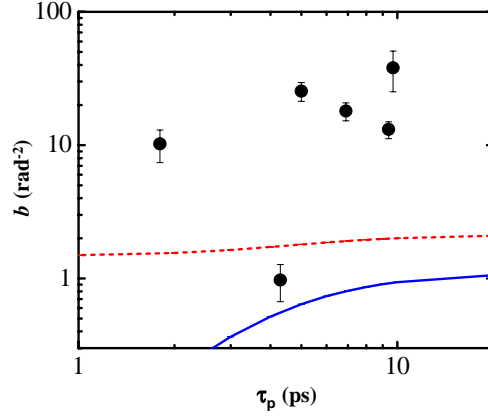
**Fig. 4.** The quadratic coefficient $b$ of the anisotropy parameter $A(\theta)$, from (3) and (4), obtained by fitting to the experimental data near the origin, and expressed as a function of the momentum scatting time $\tau_{\mathrm{p}}$. The lines show the theoretical predictions for $\eta = 2$ (*dashed line*) and $\eta = 1/2$ (*solid line*)

$$
\begin{aligned}
A(\theta) &\equiv \frac{\Delta H_{\mathrm{pp}}(\theta)}{\Delta H_{\mathrm{pp}}(0)} = \frac{1/T_2^*(\theta)}{1/T_2^*(0)} \\
&= \left[ 1 + (\omega_{\mathrm{L}} - \omega_{\mathrm{c}})^2 \, \tau_{\mathrm{p}}^2 \right] \\
&\quad \times \left[ \frac{\eta \sin^2 \theta}{1 + (\omega_{\mathrm{c}} \cos \theta)^2 \tau_{\mathrm{p}}^2} + \frac{\left(\cos^2 \theta + 1\right)/2}{1 + (\omega_{\mathrm{L}} - \omega_{\mathrm{c}} \cos \theta)^2 \tau_{\mathrm{p}}^2} \right].
\end{aligned} \tag{3}
$$

## 8 Results

In Fig. 3, we show the renormalized linewidths for all six samples, along with the theoretical results for $A(\theta)$. In five of these six cases, the experimental anisotropies at small angles clearly differ substantially from the theoretical

---

main types of asymmetries: (a) bulk inversion asymmetry (BIA) associated with the crystal lattice of the growth material [150], (b) structural inversion asymmetry (SIA) arising from explicit asymmetries in the heterostructure (e.g., dopants on the top, not the bottom) [150], (c) native interface asymmetry (NIA) arising from chemical bonds at the interface [151], and (d) fluctuations in the dopant concentration [152]. Neither (a) nor (c) are present in Si/SiGe heterostructures [153], leaving (b) and (d) as the possible sources of perpendicular electric fields. It is most likely that SIA arises from modulation doping fields, which can also lead to local fluctuations in the charge density (d).

predictions. We can quantify this difference as follows. Since (3) applies for small $\theta$, we can perform a Taylor expansion to give

$$A(\theta) = 1 + b\,\theta^2, \qquad (\theta \ll \pi/2), \tag{4}$$

where the quadratic coefficient $b$ is a measure of how quickly the anisotropy increases with angle $\theta$. For each sample, $b$ can be determined experimentally by fitting the data. A plot of $b$ as a function of the momentum relaxation time $\tau_\mathrm{p}$ is given in Fig. 4, and the results are also listed in Table 1. For all six samples, the quadratic coefficients $b$ differ substantially from the theoretical predictions, considering both proposed values of $\eta$. Even more striking, the maximum theoretical value of $b$ for any value of $\tau_\mathrm{p}$ is about $2\ \mathrm{rad}^{-2}$. This value is nearly an order of magnitude smaller than the experimental observations for five of the six samples.

As Fig. 4 demonstrates, the semi-classical expression for $1/T_{2\mathrm{R}}$ in (2) does not account for the observed behavior of $1/T_2^*$ in our samples. Various mechanisms could be contributing to the linewidth, through the component $1/T_2'$. In this case, $1/T_2'$ would necessarily contain an angular dependence, otherwise the functional form of the anisotropy would be unchanged, leaving $b$ unaffected. The observed discrepancy must therefore involve an angular dependence. Since bulk silicon possesses a crystallographic inversion symmetry, orientationally dependent mechanisms [141, 154] originating from the antisymmetric Dresselhaus term in the Hamiltonian [155], should not contribute to the linewidth.

There are several possible explanations for the observed anisotropy. In a recent paper, it was shown that in addition to the magnetic excitation mechanism, a microwave electric field may also excite ESR, as mediated by the spin-orbit coupling in a AlAs quantum well [132]. This contribution could provide an anomalous orientational dependence, since it depends only on the in-plane component of the $E$-field. However, the same mechanism has not yet been observed in Si quantum wells, where the spin-orbit coupling is very small. In our experiments, we were careful to place samples only at the zero-field nodes of the resonating cavity, so related effects would be minimized. Further, sample IBM-1 shows dramatically different orientational dependence than the other samples, yet the measurement procedure was the same for all samples. Thus, electric-field effects seem an unlikely explanation for the divergent examples of broadening observed here. It is also possible that the unexpected behavior arises from angular dependence of the inhomogeneous broadening. One could test this hypothesis by means of pulsed EPR experiments, which measure $T_2$ instead of $T_2^*$, thus removing the sensitivity to inhomogeneous broadening. The latter can arise from static dipole-dipole interactions with $^{29}$Si nuclei. Interactions with residual $^{29}$Si nuclei can also be eliminated by growing quantum wells with isotopically purified $^{28}$Si.

## 9 Conclusions

In this paper, we have reviewed the current state of silicon quantum devices and silicon ESR in 2DEGs. We have also presented results of ESR and transport measurements in a number of 2DEGs used in recent quantum device experiments. Specifically, we have analyzed the orientational dependence of the ESR linewidths. In one of our samples, we observed a dependence similar to recent observations in other groups. However, for five other samples, we observe an orientation-dependent spin decoherence with an anisotropy larger than the predictions of any current theory.

As discussed in the first half of this chapter, silicon quantum devices have advanced dramatically over the past decade, and are increasingly used in spintronics and related valley-based applications. Recent progress has demonstrated that quantum effects thought to be difficult to observe in silicon can in fact be realized, and one hopes that this will be a springboard for future work.

## Acknowledgments

## References

1. I. Žutić, J. Fabian, S. Das Sarma: Spintronics: Fundamentals and applications, Rev. Mod. Phys. **76**, 323–410 (2004)
2. S. Datta, B. Das : Electronic analog of the electro-optic modulator, Appl. Phys. Lett. **56**, 665–667 (1990)
3. M.A. Nielsen, I.L. Chuang: *Quantum computation and quantum information*, (Cambridge University, Cambridge 2000)
4. C. Poole: *Electron Spin Resonance*, 2nd Edn. (Dover, Minneola, New York 1996)
5. C.P. Slichter: *Principles of magnetic resonance*, 2nd. Edn. (Spinger-Verlag, Berlin 1978)
6. D. Stein, K. von Klitzing, G. Weimann: Electron spin resonance on GaAs-$Al_xGa_{1-x}As$ heterostructures, Phys. Rev. Lett. **51**, 130–133 (1983)
7. M. Ciorga, A.S. Sachrajda, P. Hawrylak, C. Gould, P. Zawadzki, S. Jullian, Y. Feng, Z. Wasilewski: Addition spectrum of a lateral dot from Coulomb and spin blockade spectroscopy, Phys. Rev. B **61**, R16315–R16318 (2000).
8. T. Fujisawa, D.G. Austing, Y. Tokura, Y. Hirayama, S. Tarucha: Allowed and forbidden transitions in artificial hydrogen and helium atoms, Nature (London) **419**, 278–281 (2002)
9. J.M. Elzerman, R. Hanson, L.H. Willems van Beveren, B. Witkamp, L.M.K. Vandersypen, L.P. Kouwenhoven: Single-shot read-out of an individual electron spin in a quantum dot, Nature (London) **430**, 431 (2004)

10. F.H.L. Koppens, J.A. Folk, J.M. Elzerman, R. Hanson, L.H. Willems van Beveren, I.T. Vink, H.P. Tranitz, W. Wegscheider, L.P. Kouwenhoven, L.M.K. Vandersypen: Control and detection of singlet-triplet mixing in a random nuclear field, Science **309**, 1346–1350 (2005)
11. J.R. Petta, A.C. Johnson, J.M. Taylor, E.A. Laird, A. Yacoby, M.D. Lukin, C.M. Marcus, M.P. Hanson, A.C. Gossard: Coherent manipulation of coupled electron spins in semiconductor quantum dots, Science **309**, 2180–2184 (2005)
12. A.C. Johnson, J.R. Petta, J.M. Taylor, A. Yacoby, M.D. Lukin, C.M. Marcus, M.P. Hanson, A.C. Gossard: Triplet-singlet spin relaxation via nuclei in a double quantum dot, Nature (London) **435**, 925–928 (2005)
13. R. Hanson, L.H. Willems van Beveren, I.T. Vink, J.M. Elzerman, W.J.M. Naber, F.H.L. Koppens, L.P. Kouwenhoven, L.M.K. Vandersypen: Single-shot readout of electron spin states in a quantum dot using spin-dependent tunnel rates, Phys. Rev. Lett. **94**, 196802 (2005)
14. F.H.L. Koppens, C.Buizert, K.J. Tielrooij, I.T. Vink, K.C. Nowack, T. Meunier, L.P. Kouwenhoven, L.M.K. Vandersypen: Driven coherent oscillations of a single electron spin in a quantum dot, Nature (London) **442**, 766–771 (2006)
15. T. Ando, A.B. Fowler, F. Stern: Electronic properties of two-dimensional systems, Rev. Mod. Phys. **54**, 437–672 (1982)
16. S.M. Sze: *Physics of semiconductor devices*, 2nd Edn. (Wiley, New York 1981)
17. Y. Takahashi, M. Nagase, H. Namatsu, K. Kurihara, K. Iwdate, Y. Nakajima, S. Horiguchi, K. Murase, M. Tabe: Fabrication technique for Si single-electron transistor operating at room temperature, Electron. Lett. **31**, 136–137 (1995)
18. L. Guo, E. Leobandung, L. Zhuang, S.Y. Chou: Fabrication and characterization of room temperature silicon single electron memory, J. Vac. Sci. Technol. B **15**, 2840–2843 (1997)
19. S.K. Ray, L.K. Bera, C.K. Maiti, S. John, S.K. Banerjee: Electrical characteristics of plasma oxidized $Si_{1xy}Ge_xC_y$ metaloxidesemiconductor capacitors, Appl. Phys. Lett. **72** 1250–1252 (1998)
20. D. Ali and H. Ahmed: Coulomb blockade in a silicon tunnel junction device, Appl. Phys. Lett. **64**, 2119–2120 (1994)
21. L. Guo, E. Leobandung, S.Y. Chou: A silicon single-electron transistor memory operating at room temperature, Science **275**, 649–651 (1997)
22. M. Khoury, M.J. Rack, A. Gunther, D.K. Ferry: Spectroscopy of a silicon quantum dot, Appl. Phys. Lett. **74**, 1576–1578 (1999)
23. K.-S. Park, S.-J. Kim, I.-B. Baek, W.-H. Lee, J.-S. Kang, Y.-B. Jo, S.D. Lee, C.-K. Lee, J.-B. Choi, J.-H. Kim, K.-H. Park, W.-J. Cho, M.-G. Jang, S.-J. Lee: SOI single-electron transistor with low RC delay for logic cells and SET/FET hybrid ICs, IEEE Trans. Nanotechnol. **4**, 242–248 (2005)
24. E.G. Emiroglu, D.G. Hasko, D.A. Williams: Isolated double quantum dot capacitively coupled to a single quantum dot single-electron transistor in silicon, Appl. Phys. Lett. **83**, 3942–3944 (2003)
25. S.D. Lee, K.S. Park, J.W. Park, J.B. Choi, S.-R.E. Yang, K.-H. Yoo, J. Kim, S.I. Park, K.T. Kim: Single-electron spectroscopy in a coupled triple-dot system: Role of interdot electron-electron interactions, Phys. Rev. B **62**, R7735–R7738 (2000)
26. S.D. Lee, S.J. Shin, S.J. Choi, J.J. Lee, J.B. Choi , S. Park, S.-R.E. Yang, S.J. Lee, T.H. Zyung: Si-based Coulomb blockade device for spin qubit logic gate, Appl. Phys. Lett. **89**, 023111 (2006)

27. A. Fujiwara, Y. Takahashi: Manipulation of elementary charge in a silicon charge-coupled device, Nature (London) **410**, 560–562 (2001)
28. J. Gorman, D.G. Hasko, D.A. Williams: Charge-qubit operation of an isolated double quantum dot, Appl. Phys. Lett. **95**, 090502 (2005)
29. K. Takashina, Y. Ono, A. Fujiwara, Y. Takahashi, Y. Hirayama: Valley polarization in Si(100) at zero magnetic field, Phys. Rev. Lett. **96**, 236801 (2006)
30. T. Ouisse, D.K. Maude, S. Horiguchi, Y. Ono, Y. Takahashi, K. Murase, S. Cristoloveanu: Subband structure and anomalous valley splitting in ultra-thin silicon-on-insulator MOSFET's, Physica B (Amsterdam) **249–251**, 731–734 (1998)
31. R. Augke, W. Eberhardt, C. Single, F.E. Prins, D.A. Wharam, D.P. Kern: Doped silicon single electron transistors with single island characteristics, Appl. Phys. Lett. **76**, 2065–2067 (2000)
32. N.M. Zimmerman. W.H. Huber, A. Fujiwara, Y. Takahashi: Excellent charge offset stability in a Si-based single-electron tunneling transistor, Appl. Phys. Lett. **79**, 3188–3190 (2001)
33. J.H.F. Scott-Thomas, S.B. Field, M.A. Kastner, H.I. Smith, D.A. Antoniadia: Conductance oscillations periodic in the density of a one-dimensional electron gas, Phys. Rev. Lett. **62**, 583–586 (1989)
34. R.A. Smith, H. Ahmed: Gate controlled Coulomb blockade effects in the conduction of a silicon quantum wire, J. Appl. Phys. **81**, 2699–2703 (1997)
35. L.P. Rokhinson, L.J. Guo, S.Y. Chou, D.C. Tsui: Double-dot charge transport in Si single-electron/hole transistors, Appl. Phys. Lett. **76**, 1591–1593 (2000)
36. B.H. Choi, Y.S. Yu, D.H. Kim, S.H. Son, K.H. Cho, S.W. Hwang, D. Ahn, B.-G. Park: Double-dot-like charge transport through a small size silicon single electron transistor, Physica E (Amsterdam) **13**, 946–949 (2002)
37. K.H. Cho, B.H. Choi, S.H. Son, S.W. Hwang , D. Ahn, B.-G. Park, B. Naser, J.-F. Lin, J.P. Bird: Evidence of double layer quantum dot formation in a silicon-on-insulator nanowire transistor, Appl. Phys. Lett. **86**, 043101 (2005)
38. Y. Ono, A. Fujiwara, K. Nishiguchi, H. Inokawa, Y. Takahashi: Manipulation and detection of single electrons for future information processing, J. Appl. Phys. **97**, 031101 (2005)
39. F. Schäffler: High-mobility Si and Ge structures, Semicond. Sci. Technol. **12**, 1515–1549 (1997)
40. B.S. Meyerson: UHV/CVD growth of Si and Si:Ge alloys: chemistry, physics, and device applications, Proc. IEEE **80**, 1592–1608 (1992)
41. P.A. Cain, H. Ahmed, D.A. Williams, J.M. Bonar: Hole transport through single and double SiGe quantum dots, Appl. Phys. Lett. **77**, 3415–3417 (2000)
42. P.A. Cain, H. Ahmed, D.A. Williams: Conductance peak splitting in hole transport through a SiGe double quantum dot, Appl. Phys. Lett. **78**, 3624–3626 (2001)
43. P.A. Cain. H. Ahmed , D.A. Williams: Hole transport in coupled SiGe quantum dots for quantum computation, Journ. Appl. Phys. **92**, 346–350 (2002)
44. H. Qin, S. Yasin, D.A. Williams: Fabrication and characterization of a SiGe double quantum dot structure, J. Vac. Sci. Technol. B **21**, 2852–2855 (2003)
45. D.S. Gandolfo, D.A. Williams, H. Qin: Characterization of a silicon-germanium quantum dot structure at 4.2 K and 40 mK, Journ. Appl. Phys. **97**, 063710 (2005)

46. S.F. Nelson, K. Ismail, J.J. Nocera, F.F. Fang, E.E. Mendez, J.O. Chu, B.S. Meyerson: Observation of the fractional quantum Hall effect in Si/SiGe heterostructures, Appl. Phys. Lett. **61** 64–66 (1992)

47. K. Ismail, J.O. Chu, K.L. Saenger, B.S. Meyerson, W. Rausch: Modulation-doped $n$-type Si/SiGe with inverted interface, Appl. Phys. Lett. **65**, 1248–1250 (1994)

48. K. Ismail, M. Arafa, K.L. Saenger, J.O. Chu, B.S. Meyerson: Extremely high electron mobility in Si/SiGe modulation-doped heterostructures, Appl. Phys. Lett. **66**, 1077–1079 (1995)

49. L. Di Gaspare, K. Alfaramawi, F. Evangelisti, E. Palange, G. Barucca G, G. Majni: Si/SiGe modulation-doped heterostructures grown on silicon-on-insulator substrates for high-mobility two-dimensional electron gases, Appl. Phys. Lett. **79**, 2031–2033 (2001)

50. T. Okamoto, M. Ooya, K. Hosoya, S. Kawaji: Spin polarization and metallic behavior in a silicon two-dimensional electron system, Phys. Rev. B **69**, 041202 (2004)

51. F. Stern, S.E. Laux: Charge transfer and low-temperature electron mobility in a strained Si layer in relaxed $Si_{1x}Ge_x$, Appl. Phys. Lett. **61**, 1110–1112 (1992)

52. D. Monroe, Y.H. Xie, E.A. Fitzgerald, P.J. Silverman, G.P. Watson: Comparison of mobility-limiting mechanisms in high-mobility $Si_{1-x}Ge_x$ heterostructures, J. Vac. Sci. Technol. **11**, 1731–1737 (1993)

53. M.A. Eriksson, M. Friesen, S.N. Coppersmith, R. Joynt, L.J. Klein, K. Slinker, C. Tahan, P.M. Mooney, J.O. Chu, S.J. Koester: Spin-based quantum dot quantum computing in silicon, Quant. Inform. Process. **3**, 133–146 (2004)

54. W.X. Gao, K. Ismail, K.Y. Lee, J.O. Chu, S. Washburn: Observation of ballistic conductance and Aharonov-Bohm oscillations in Si/SiGe heterostructures, Appl. Phys. Lett. **65**, 3114–3116 (1994)

55. S.J. Koester, K. Ismail, K.Y. Lee, J.O. Chu: Negative differential conductance in strained Si point contacts and wires, Appl. Phys. Lett. **71**, 1528–1530 (1997)

56. L.P. Kouwenhoven, C.M. Marcus, P.L. McEuen, S. Tarucha, R.M. Westervelt, N.S. Wingreen: Electron transport in quantum dots in L.L. Sohn, L.P. Kouwenhoven, G. Schön (Eds.): Mesoscopic Electron Transport (Kluwer, Dordrecht 1997), pp. 105–214

57. L.J. Klein, K.A. Slinker, J.L. Truitt, S. Goswami, K.L.M. Lewis, S.N. Coppersmith, D.W. van der Weide, M. Friesen, R.H. Blick, D.E. Savage, M.G. Lagally, C. Tahan, R. Joynt, M.A. Eriksson, J.O. Chu, J.A. Ott, P.M. Mooney: Coulomb blockade in a silicon/silicon-germanium two-dimensional electron gas quantum dot, Appl. Phys. Lett. **84**, 4047–4049 (2004)

58. S. Kanjanachuchai, T.J. Thornton, J.M. Fernández, H. Ahmed H: Coulomb blockade in strained-Si nanowires on leaky virtual substrates, Semicond. Sci. Technol. **16**, 72–76 (2001)

59. T. Berer, D. Pachinger, G. Pillwein, M. Mühlberger, H. Lichtenberger, G. Brunthaler, F. Schäffler: Lateral quantum dots in Si/SiGe realized by a Schottky split-gate technique, Appl. Phys. Lett. **88**, 162112 (2006)

60. S.J Koester, K. Ismail, K.Y. Lee, J.O. Chu: Weak localization in back-gated $Si/Si_{0.7}Ge_{0.3}$ quantum-well wires fabricated by reactive ion etching, Phys. Rev. B **54**, 10604–10608 (1996)

61. K.Y. Lee, S.J. Koester, K. Ismail, J.O. Chu: Electrical characterization of $Si/Si_{0.7}Ge_{0.3}$ quantum well wires fabricated by low damage $CF_4$ reactive ion etching, Microelectron. Eng. **35**, 33–36 (1997)

62. L.J. Klein, K.L.M. Lewis, K.A. Slinker, S. Goswami, D.W. van der Weide, R.H. Blick, P.M. Mooney, J.O. Chu, S.N. Coppersmith, M. Friesen, M.A. Eriksson: Quantum dots and etch-induced depletion of a silicon two-dimensional electron gas, J. Appl. Phys. **99**, 023509 (2006)

63. M. Holzmann, D. Többen, G. Abstreiter, M. Wendel, H. Lorenz, J.P. Kotthaus, F. Schäffler: One-dimensional transport of electrons in $Si/Si_{0.7}Ge_{0.3}$ heterostructures, Appl. Phys. Lett. **66**, 833–835 (1995)

64. R.G. Van Veen, A.H. Verbruggen, E. van der Drift, F. Schäffler, S. Radelaar: Experimental study on magnetoresistance phenomena in $n$-type Si/SiGe quantum wires, Semicond. Sci. Technol. **14**, 508–516 (1999)

65. E. Giovine, A. Notargiacomo1, L. Di Gaspare, E. Palange, F. Evangelisti, R. Leoni, G. Castellano, G. Torrioli, V. Foglietti: Investigation of SiGe-heterostructure nanowires, Nanotechnol. **12**, 132–135 (2001)

66. U. Wieser, U. Kunze, K. Ismail, J.O. Chu JO: Fabrication of Si/SiGe quantum point contacts by electron-beam lithography and shallow wet-chemical etching, Physica E (Amsterdam) **13**, 1047–1050 (2002)

67. U. Dötsch, U. Gennser, C. David, G. Dehlinger, D. Grützmacher, T. Heinzel, S. Lüscher, K. Ensslin: Single-hole transistor in a $p$-Si:SiGe quantum well, Appl. Phys. Lett. **78**, 341–343 (2001)

68. A. Notargiacomo, L. Di Gaspare, G. Scappucci, G. Mariottini, F. Evangelisti, E. Giovine, R. Leoni: Single-electron transistor based on modulation-doped SiGe heterostructures, Appl. Phys. Lett. **83**, 302–304 (2003)

69. M.R. Sakr, H.W. Jiang, E. Yablonovitch, E.T. Croke: Fabrication and characterization of electrostatic Si/SiGe quantum dots with an integrated read-out channel, Appl. Phys. Lett. **87**, 223104 (2005)

70. M. Holzmann, D. Többen, G. Abstreiter, F. Schäffler: Field-effect induced electron channels in a $Si/Si_{0.7}Ge_{0.3}$ heterostructure, J. Appl. Phys. **76**, 3917–3919 (1994)

71. R.B. Dunford, N. Griffin, D.J. Paul, M. Pepper, D.J. Robbins, A.C. Churchill, W.Y. Leong: Schottky gating high mobility $Si/Si_{1-x}Ge_x$ 2D electron systems, Thin Solid Films **369**, 316–319 (2000)

72. K.A. Slinker, K.L.M. Lewis, C.C. Haselby, S. Goswami, L.J. Klein, J.O. Chu, S.N. Coppersmith, R. Joynt, R.H. Blick, M. Friesen, M.A. Eriksson: Quantum dots in Si/SiGe 2DEGs with Schottky top-gated leads, New Journ. Phys. **7**, 246 (2005)

73. L.J. Klein, D.E. Savage, M.A. Eriksson: Coulomb blockade and Kondo effect in a few-electron silicon/silicon-germanium quantum dot, Appl. Phys. Lett. **90**, 033103 (2007)

74. T. Berer, D. Pachinger, G. Pillwein, M. Mühlberger, H. Lichtenberger, G. Brunthaler, F. Schäffler: Single-electron transistor in strained Si/SiGe heterostructures, Physica E (Amsterdam) **34**, 456–459 (2006)

75. D. Többen, D.A. Wharam, G. Abstreiter, J.P. Kotthaus, F. Schäffler F: Transport properties of a Si/SiGe quantum point contact in the presence of impurities, Phys. Rev. B **52**, 4704–4707 (1995)

76. D. Többen, D.A. Wharam, G. Abstreiter, J.P. Kotthaus, F. Schäffler F: Ballistic electron transport through a quantum point contact defined in a $Si/Si_{0.7}Ge_{0.3}$ heterostructure, Semicond. Sci. Technol. **10**, 711–714 (1995)

77. G. Scappucci, L. Di Gaspare, E. Giovine, A. Notargiacomo, R. Leoni, F. Evangelisti: Conductance quantization in etched Si/SiGe quantum point contacts, Phys. Rev. B **74**, 035321 (2006)

78. G.D. Scott, M. Xiao, H.W. Jiang, E.T. Croke, E. Yablonovitch: Sputtered gold as an effective Schottky gate for strained Si/SiGe nanostructures, Appl. Phys. Lett. **90**, 032110 (2007)
79. S. Goswami, K.A. Slinker, M. Friesen, L.M. McGuire, J.L. Truitt, C. Tahan, L.J. Klein, J.O. Chu, P.M. Mooney, D.W. van der Weide, R. Joynt, S.N. Coppersmith, M.A. Eriksson: Controllable valley splitting in silicon quantum devices, Nature Phys. **3**, 41–45 (2007)
80. M.M. Roberts, L.J. Klein, D.E. Savage, K.A. Slinker, M. Friesen, G. Celler, M.A. Eriksson, M.G. Lagally: Elastically relaxed free-standing strained-silicon nanomembranes, Nature Mater. **5**, 388–393 (2006)
81. P. Zhang, E.P. Nordberg, B.-N. Park, G.K. Celler, I. Knezevic, P.G. Evans, M.A. Eriksson, M.G. Lagally: Electrical conductivity in silicon nanomembranes, New J. Phys. **8**, 200 (2006)
82. D. Loss, D.P. DiVincenzo: Quantum computation with quantum dots, Phys. Rev. A **57**, 120–126 (1998)
83. V. Cerletti, W.A. Coish, O. Gywat, D. Loss: Recipes for spin-based quantum computing, Nanotechnol. **16**, R27–R49 (2005)
84. B.E. Kane: A silicon-based nuclear spin quantum computer, Nature (London) **393**, 133–137 (1998)
85. J.L. O'Brien, S.R. Schofield, M.Y. Simmons, R.G. Clark, A.S. Dzurak, N.J. Curson, B.E. Kane, N.S. McAlpine, M.E. Hawley, G.W. Brown: Towards the fabrication of phosphorus qubits for a silicon quantum computer, Phys. Rev. B **64**, 161401 (2001)
86. G. Berman, G.W. Brown, M.E. Hawley, V.I. Tsifrinovich: Solid-state quantum computer based on scanning tunneling microscopy, Phys. Rev. Lett. **87**, 097902 (2001)
87. T.D. Ladd, J.R. Goldman, F. Yamaguchi, Y. Yamamoto, E. Abe, K.M. Itoh: All-silicon quantum computer, Phys. Rev. Lett. **89**, 017901 (2002)
88. T. Schenkel, A. Persaud, S.J. Park, J. Nilsson, J. Bokor, J.A. Liddle, R. Keller, D.H. Schneider, D.W. Cheng, D.E. Humphries: Solid state quantum computer development in silicon with single ion implantation, J. Appl. Phys. **94**, 7017–7024 (2003)
89. R.G. Clark, R. Brenner, T.M. Buehler, V. Chan, N.J. Curson, A.S. Dzurak, E. Gauja, H.S. Goan, A.D. Greentree, T. Hallam, A.R. Hamilton, L.C.L. Hollenberg, D.N. Jamieson, J.C. McCallum, G.J. Milburn, J.L. O'Brien, L. Oberbeck, C.I. Pakes, S.D. Prawer, D.J. Reilly, F.J. Ruess, S.R. Schofield, M.Y. Simmons, F.E. Stanley, R.P. Starrett, C. Wellard, C. Yang: Progress in silicon-based quantum computing, Philos. Trans. R. Soc. Lond., Ser. A **361**, 1451–1471 (2003)
90. A.J. Skinner, M.E. Davenport, B.E. Kane: Hydrogenic spin quantum computing in silicon: A digital approach, Phys. Rev. Lett. **90**, 087901 (2003)
91. A.M. Stoneham, A.J. Fisher, P.T. Greenland: Optically driven silicon-based quantum gates with potential for high-temperature operation, J. Phys.: Condens. Matter **15**, L447–L451 (2003)
92. C.D. Hill, L.C.L. Hollenberg, A.G. Fowler, C.J. Wellard, A.D. Greentree, H.-S. Goan: Global control and fast solid-state donor electron spin quantum computing, Phys. Rev. B **72**, 045350 (2005)
93. T.M. Buehler, V. Chan, A.J. Ferguson, A.S. Dzurak, F.E. Hudson, D.J. Reilly, A.R. Hamilton, R.G. Clark, D.N. Jamieson, C. Yang, C.I. Pakes, S. Prawer: Controlled single electron transfer between Si:P dots, Appl. Phys. Lett. **88**, 192101 (2006)

94. R. Vrijen, E. Yablonovitch, K. Wang, H.W. Jiang, A. Balandin, V. Roychowd-hury, T. Mor, D. DiVincenzo: Electron-spin-resonance transistors for quantum computing in silicon-germanium heterostructures, Phys. Rev. A **62**, 012306 (2000)
95. J. Levy: Quantum-information processing with ferroelectrically coupled quantum dots, Phys. Rev. A **64**, 052306 (2001)
96. M. Friesen, P. Rugheimer, D.E. Savage, M.G. Lagally, D.W. van der Weide, R. Joynt, M.A. Eriksson: Practical design and simulation of silicon-based quantum-dot qubits, Phys. Rev. B **67**, 121301(R) (2003)
97. J.P. Gordon, K.D. Bowers: Microwave spin echoes from donor electrons in silicon, Phys. Rev. Lett. **1**, 368–370 (1958)
98. E. Abe, K.M. Itoh, J. Isoya, S. Yamasaki: Electron-spin phase relaxation of phosphorus donors in nuclear-spin-enriched silicon, Phys. Rev. B **70**, 033204 (2004)
99. A.M. Tyryshkin, S.A. Lyon, A.V. Astashkin, A.M. Raitsimring: Electron spin relaxation times of phosphorus donors in silicon, Phys. Rev. B **68**, 193207 (2003)
100. M. Xiao, I. Martin, E. Yablonovitch, H.W. Jiang: Electrical detection of the spin resonance of a single electron in a silicon field-effect transistor, Nature (London) **430**, 435–439 (2004)
101. M. Friesen, S. Chutia, C. Tahan, S.N. Coppersmith: Valley Splitting Theory of SiGe/Si/SiGe Quantum Wells, to appear in Phys. Rev. B, cond-mat/0608229 (unpublished)
102. L.J. Sham, M. Nakayama: Effective-mass approximation in the presence of an interface, Phys. Rev. B **20**, 734–747 (1979)
103. F.J. Ohkawa, Y. Uemura: Theory of valley splitting in an $N$-Channel (100) inversion layer of Si: I. Formulation by extended zone effective mass theory, J. Phys. Soc. Japan **43**, 907–916 (1977)
104. F.J. Ohkawa, Y. Uemura: Theory of valley splitting in an $N$-Channel (100) Inversion Layer of Si: II. Electric Break Through, J. Phys. Soc. Japan **43**, 917–924 (1977)
105. F.J. Ohkawa: Electric break-through in an inversion layer: Exactly solvable model, Solid State Commun. **26**, 69–71 (1978)
106. H. Fritzsche: Effect of stress on the donor wave functions in germanium, Phys. Rev. **125**, 1560–1567 (1962)
107. W.D. Twose, in the Appendix of [106]
108. M. Nakayama, L.J. Sham: Surface-induced valley-splitting in $n$-channel (001) silicon-MOS charge layer, Solid State Commun. **28**, 393–396 (1978)
109. F.J. Ohkawa: Multi-valley effective mass theory, J. Phys. Soc. Japan **46**, 736–743 (1979)
110. T.B. Boykin, G. Klimeck, M.A. Eriksson, M. Friesen, S.N. Coppersmith, P. von Allmen, F. Oyafuso, S. Lee: Valley splitting in strained silicon quantum wells, Appl. Phys. Lett. **84**, 115–117 (2004)
111. T.B. Boykin, G. Klimeck, M. Friesen, S.N. Coppersmith, P. von Allmen, F. Oyafuso, S. Lee: Valley splitting in low-density quantum-confined heterostructures studied using tight-binding models, Phys. Rev. B **70**, 165325 (2004)
112. T.B. Boykin, G. Klimeck, P. von Allmen, S. Lee, F. Oyafuso: Valley splitting in V-shaped quantum wells, J. Appl. Phys. **97**, 113702 (2005)
113. M.O. Nestoklon, L.E. Golub, E.L. Ivchenko: Spin and valley-orbit splittings in SiGe/Si heterostructures, Phys. Rev. B **73**, 235334 (2006)

114. M. Friesen, M.A. Eriksson, S.N. Coppersmith: Magnetic field dependence of valley splitting in realistic Si/SiGe quantum wells, Appl. Phys. Lett. **89**, 202106 (2006)

115. P. Weitz, R.J. Haug, K. von Klitzing, F. Schäffler: Tilted magnetic field studies of spin- and valley-splittings in $Si/Si_{1-x}Ge_x$ heterostructures, Surf. Sci. **361–362**, 542–546 (1996)

116. S.J. Koester, K. Ismail, J.O. Chu: Determination of spin- and valley-split energy levels in strained Si quantum wells, Semicond. Sci. Technol. **12**, 384–388 (1997)

117. H.W. Schumacher, A. Nauen, U. Zeitler, R.J. Haug, P. Weitz, A.G.M. Jansen, F. Schäffler: Anomalous coincidences between valley split Landau levels in a Si/SiGe heterostructure, Physica B (Amsterdam) **256–258**, 260–263 (1998)

118. V.S. Khrapai, A.A. Shashkin, V.P. Dolgopolov: Strong enhancement of the valley splitting in a two-dimensional electron system in silicon, Phys. Rev. B **67**, 113305 (2003)

119. K. Lai, W. Pan, D.C. Tsui, S. Lyon, M. Mühlberger, F. Schäffler: Two-flux composite fermion series of the fractional quantum hall states in strained Si, Phys. Rev. Lett. **93**, 156805 (2004)

120. M.A. Wilde, M. Rhode, C. Heyn, D. Heitmann, D. Grundler, U. Zeitler, F. Schäffler, R.J. Haug: Direct measurements of the spin and valley splittings in the magnetization of a Si/SiGe quantum well in tilted magnetic fields, Phys. Rev. B **72**, 165429 (2005)

121. K. Lai, W. Pan, D.C. Tsui, S. Lyon, M. Mühlberger, F. Schäffler: Intervalley gap anomaly of two-dimensional electrons in silicon, Phys. Rev. Lett. **96**, 076805 (2006)

122. K. Lai, T.M. Lu, W. Pan, D.C. Tsui, S. Lyon, J. Liu, Y.H. Xie, M. Mühlberger, F. Schäffler: Valley splitting of $Si/Si_{1-x}Ge_x$ heterostructures in tilted magnetic fields, Phys. Rev. B **73**, 161301 (2006)

123. T. Ando: Valley splitting in the silicon inversion layer: Misorientation effects, Phys. Rev. B **19**, 3089–3095 (1979)

124. S. Lee, P. von Allmen: Magnetic-field dependence of valley splitting in Si quantum wells grown on tilted SiGe substrates, Phys. Rev. B **74**, 245302 (2006)

125. P. von Allmen, S. Lee: Zero valley splitting at zero magnetic field for strained Si/SiGe quantum wells grown on tilted substrates, cond-mat/0606395 (unpublished)

126. K. Takashina, A. Fujiwara, S. Horiguchi, Y. Takahashi, Y. Hirayama: Valley splitting control in $SiO_2/Si/SiO_2$ quantum wells in the quantum Hall regime, Phys. Rev. B **69**, 161304(R) (2004)

127. M. D'yakonov, V. Perel': Spin relaxation of conduction electrons in noncentrosymmetric semiconductors, Sov. Phys. Solid State **13**, 3023–3026 (1972)

128. Reviewed in F. Meier, B.P. Zakharchenya (Eds.): Optical Orientation, Modern Problems in Condensed Matter Physics, vol. 8 (North-Holland, Amsterdam 1984)

129. J.M. Kikkawa, D.D. Awschalom: Resonant spin amplification in $n$-type GaAs, Phys. Rev. Lett. **80**, 4313–4316 (1998)

130. W.O. Putikka, R. Joynt: Theory of optical orientation in $n$-type semiconductors, Phys. Rev. B **70**, 113201 (2004)

131. N. Nestle, G. Denninger, M. Vidal, C. Weinzierl, K. Brunner, K. Eberl, K. von Klitzing: Electron spin resonance on a two-dimensional electron gas, Phys. Rev. B **56**, R4359–R4362 (1997)

132. M. Schulte, J.G.S. Lok, G. Denninger, W. Dietsche: Electron spin resonance on a two-dimensional electron gas in a single AlAs quantum well, Phys. Rev. Lett. **94**, 137601 (2005)
133. C.F.O. Graeff, M.S. Brandt, M. Stutzmann, M. Holzmann, G. Arbstreiter, F. Schäffler: Electrically detected magnetic resonance of two-dimensional electron gases in Si/SiGe heterostructures, Phys. Rev. B **59**, 13242–13250 (1999)
134. J. Matsunami, M. Ooya, T. Okamoto: Electrically detected electron spin resonance in a high-mobility silicon quantum well, Phys. Rev. Lett. **97**, 066602 (2006)
135. W. Jantsch, Z. Wilamowski, N. Sandersfeld, F. Schäffler: ESR investigations of modulation-doped Si/SiGe quantum wells, Phys. Stat. Sol. **210**, 643–648 (1999)
136. W. Jantsch, Z. Wilamowski, N. Sandersfeld, F. Schäffler: Electric and magnetic field fluctuations in modulation doped Si/Ge quantum wells, Physica E (Amsterdam) **6**, 218–221 (2000)
137. N. Sandersfeld, W. Jantsch, Z. Wilamowski, F. Schäffler: ESR investigation of modulation-doped Si/SiGe quantum wells, Thin Solid Films **369**, 312–315 (2000)
138. Z. Wilamowski, N. Sandersfeld, W. Jantsch, D. Többen, F. Schäffler: Screening breakdown on the route toward the metal-insulator transition in modulation doped Si/SiGe quantum wells, Phys. Rev. Lett. **87**, 026401 (2001)
139. Z. Wilamowski, W. Jantsch, H. Malissa, U. Rössler: Evidence and evaluation of the Bychkov-Rashba effect in SiGe/Si/SiGe quantum wells, Phys. Rev. B **66**, 195315 (2002)
140. Z. Wilamowski, W. Jantsch: ESR studies of the Bychkov-Rashba field in modulation doped Si/SiGe quantum wells, Physica E (Amsterdam) **12**, 439–442 (2002)
141. Z. Wilamowski, W. Jantsch: Suppression of spin relaxation of conduction electrons by cyclotron motion, Phys. Rev. B **69**, 035328 (2004)
142. Z. Wilamowski, W. Jantsch: Spin relaxation of 2D electron in Si/SiGe quantum well suppressed by applied magnetic field, Semicond. Sci. Technol. **19**, S390–S391 (2004)
143. H. Malissa, W. Jantsch, M. Mühlberger, F. Schäffler, Z. Wilamowski, M. Draxler, P. Bauer: Anisotropy of $g$-factor and electron spin resonance linewidth in modulation doped SiGe quantum wells, Appl. Phys. Lett. **85**, 1739–1741 (2004)
144. W. Jantsch, H. Malissa, Z. Wilamowski, H. Lichtenberger, G. Chen, F. Schäffler, G. Bauer: Spin properties of electrons in low-dimensional SiGe structures, Journ. Supercond. **18**, 145–149 (2005)
145. Z. Wilamowski, H. Malissa, F. Schäffler, W. Jantsch: $g$-factor tuning and manipulation of spins by an electric current, cond-mat/0610046 (unpublished)
146. A.M. Tyryshkin, S.A. Lyon, W. Jantsch, F. Schäffler: Spin manipulation of free two-dimensional electrons in Si/SiGe quantum wells, Phys. Rev. Lett. **94**, 126802 (2005)
147. M.J. Kane, N. Apsley, D.A. Anderson, L.L. Taylor, T. Kerr: Parallel conduction in GaAs/Al$_x$Ga$_{1-x}$As modulation doped heterojunctions, J. Phys. C **18**, 5629–5636 (1985)
148. G. Feher: Electron spin resonance experiments on donors in silicon. I. Electronic structure of donors by the electron nuclear double resonance technique, Phys. Rev. **114**, 1219–1244 (1959)

149. C. Tahan, R. Joynt: Rashba spin-orbit coupling and spin relaxation in silicon quantum wells, Phys. Rev. B **71**, 075315 (2005)

150. P. Pfeffer, W. Zawadzki: Spin splitting of conduction subbands in III-V heterostructures due to inversion asymmetry, Phys. Rev. B **59**, R5312–R5315 (1999)

151. J.T. Olesberg, W.H. Lau, M.E. Flatté, C. Yu, E. Altunkaya, E.M. Shaw, T.C. Hasenberg, T.F. Boggess: Interface contributions to spin relaxation in a short-period InAs/GaSb superlattice, Phys. Rev. B **64**, 201301(R) (2001)

152. E.Y. Sherman: Random spinorbit coupling and spin relaxation in symmetric quantum wells, Appl. Phys. Lett. **82**, 209–211 (2003)

153. E.Y. Sherman: Minimum of spin-orbit coupling in two-dimensional structures, Phys. Rev. B **67**, 161303(R) (2003)

154. E.L. Ivchenko: Spin relaxation of free carriers in a noncentrosymmetric semiconductor in a longitudinal magnetic field, Sov. Phys. Solid State **15**, 1048–1050 (1973)

155. G. Dresselhaus: Spin-orbit coupling effects in zinc blende structures, Phys. Rev. **100**, 580–586 (1955)